Acta Materialia 108 (2016) 293–303

Contents lists available at ScienceDirect

Acta Materialia

journal homepage: www.elsevier.com/locate/actamat

Full length article

New nanostructured phases with reversible hydrogen storage capability in immiscible magnesium–zirconium system produced by high-pressure torsion

Kaveh Edalati [a, b, *], Hoda Emami [a], Yuji Ikeda [c], Hideaki Iwaoka [b], Isao Tanaka [c, d], Etsuo Akiba [a, e], Zenji Horita [a, b]

[a] *WPI, International Institute for Carbon-Neutral Energy Research (WPI-I2CNER), Kyushu University, Fukuoka, 819-0395, Japan*
[b] *Department of Materials Science and Engineering, Faculty of Engineering, Kyushu University, Fukuoka, 819-0395, Japan*
[c] *Center for Elements Strategy Initiative for Structure Materials (ESISM), Kyoto University, Sakyo, Kyoto, 606-8501, Japan*
[d] *Department of Materials Science and Engineering, Kyoto University, Kyoto, 606-8501, Japan*
[e] *Department of Mechanical Engineering, Faculty of Engineering, Kyushu University, Fukuoka, 819-0395, Japan*

ARTICLE INFO

Article history:
Received 16 January 2016
Received in revised form
10 February 2016
Accepted 10 February 2016

Keywords:
Mg-Zr phase diagram
Phase transformations
Metal hydrides
Mechanical alloying
Density functional theory (DFT)

ABSTRACT

Mg and Zr are immiscible in the solid and liquid states and do not form any binary phases. In this study, Mg and Zr were significantly dissolved in each other by severe plastic deformation (SPD) through the high-pressure torsion (HPT) method and several new metastable phases were formed: nanostructured hcp, nano-twinned fcc, bcc or ordered bcc-based phases. These supersaturated Mg–Zr phases, which did not decompose up to 773 K, exhibited reversible hydrogen storage capability at room temperature. They absorbed ~1 wt.% of hydrogen under 9 MPa in ~20 s and fully desorbed the hydrogen in the air. First-principles phonon calculations revealed that the disordered hcp and fcc solid solutions were dynamically stable in the whole composition range of the Mg–Zr system. The bcc or bcc-based ordered phases, which were formed only as intermediate phases during the phase transformation to the hcp solid solution alloy, were energetically higher and were dynamically stable only under limited conditions in the Mg-rich compositions.

1. Introduction

Phase transformations in the Mg–Zr system has not been investigated significantly because Mg and Zr are immiscible in the solid state as well as in the liquid state [1]. Although both Mg and Zr have the hcp structures with nearly similar lattice parameters at ambient pressure and room temperature, earlier experimental and theoretical studies confirmed that no binary phases can be formed in the Mg–Zr equilibrium phase diagram [1–3]. So far, there have been few attempts to examine the formation of non-equilibrium (metastable) phases in the Mg–Zr system.

Mg can store hydrogen in the form of MgH_2 and Zr, which belongs to the group 4 of the periodic table (Ti, Zr and Hf), can also store hydrogen in the form of ZrH_2. Although the hydrogen storage performance of the Mg–Ti–H system has been investigated significantly (e.g., see Refs. [4–11]), there have been limited attempts to examine the hydrogen storage performance of the Mg–Zr–H system [8–18]. Goto et al. [12] and Okada et al. [13] employed a cubic-anvil-type apparatus and synthesized hydrides $MgZr_2H_y$ or $Mg_2Zr_3H_y$ with the monoclinic structure by processing $MgH_2 + ZrH_2$ mixture under a hydrogen pressure of 2–5 GPa at 1073–1173 K for 2 h. Takasaki et al. [14], Kyoi et al. [15] and Moser et al. [16] employed a high-pressure cell and synthesized a hydride $Mg_{0.82}Zr_{0.18}H_2$ with the fcc structure by processing a mixture of MgH_2 and ZrH_2 under a hydrogen pressure of 4–8 GPa at 873 K for 1 h. Bao et al. [17] synthesized thin film of $Mg_{0.82}Zr_{0.18}H_2$ with the fcc structure by co-sputtering of Mg and Zr followed by hydrogenation. Guzik et al. [18] conducted reactive ball milling on Mg + Zr powder mixtures under a deuterium pressure of 5.6–6.7 MPa, and synthesized a hydride $Mg_{0.40}Zr_{0.60}D_{1.78}$ with the fcc structure. First-principles calculations suggested that when the fraction of Zr in $Mg_{1-y}Zr_yH_2$ is higher than ~13 at%, a ternary hydride with the fcc crystal structure (fluorite-type structure) should be formed [19].

---

[*] Corresponding author. WPI, International Institute for Carbon-Neutral Energy Research (WPI-I2CNER), Kyushu University, Fukuoka, 819-0395, Japan.
E-mail address: kaveh.edalati@zaiko6.zaiko.kyushu-u.ac.jp (K. Edalati).

http://dx.doi.org/10.1016/j.actamat.2016.02.026
1359-6454/© 2016 Acta Materialia Inc. Published by Elsevier Ltd. All rights reserved.

In this study, formation of new metastable phases (disordered hcp, partially ordered bcc and disordered fcc) in the Mg–Zr system and their hydrogen storage performance are examined by experiments using the high-pressure torsion (HPT) method [20–22] and by first-principles calculations. The HPT method, which was first introduced by Bridgman in 1935 [23], is employed for mixing Mg and Zr in the atomic scale. Although the HPT method is currently used mainly as a severe plastic deformation (SPD) technique for grain refinement in metallic materials [24–26], there have been long-time historical efforts from 1935 [23] to now [27–29] to synthesize metastable phases by HPT processing (see a review in Ref. [30]). The HPT method was employed in this study not only because of its capability to control phase transformations [23–30], but also because of its effectiveness to activate hydrogen storage materials [31–33], increase the hydrogenation kinetics [34–38] and synthesize Mg-based hydrogen storage materials [39,40].

2. Experimental materials and methods

The Mg and Zr elements in the powder form with high purity (99.5%) and particle sizes smaller than ~44 μm (325 mesh) were mechanically mixed. The HPT process was carried out on the powder mixtures using a pair of Bridgman anvils [23], having flat-bottom holes of 14 mm diameter and 0.4 mm depth on the surface. The powder mixtures were processed by torsional straining using HPT ($\gamma = 2\pi rN/h$, γ: shear strain, r: distance from disc center, N: number of HPT turns, h: thickness of disc [20,21]) for $N = 1, 10, 100$ and 1000 turns under a pressure of $P = 1.5$ GPa with a rotation speed of $\omega = 1$ rpm at room temperature. The HPT-processed discs with 14 mm diameter were examined using various experimental methods as explained below.

In order to examine the microstructural homogeneity along the disc radii, the HPT-processed discs were first mechanically polished and the Vickers microhardness was measured using an applied load of 200 g for 15 s in three radial directions from the disc center to periphery.

Second, the microscopic distribution of elements was examined using scanning electron microscopy (SEM) equipped with energy dispersive X-ray spectroscopy (EDS). The SEM and EDS examinations were performed under an accelerating voltage of 15 kV at 4–6 mm away from the disc center.

Third, the formation of new phases was examined using X-ray diffraction (XRD) analyses using the Cu Kα radiation. Examinations were performed on the periphery of all discs as well as on the center of discs processed for $N = 100$ and 1000 turns. The XRD profiles were analyzed in details by Rietveld refinement using the FullProf Suite software [41,42].

Fourth, for microstructural examinations, transmission electron microscopy (TEM) and Cs-corrected scanning transmission microscopy (STEM) were conducted using accelerating voltages of 300 kV and 200 kV, respectively. Thin foils were prepared from 6 mm away from the disc center using a focused ion beam system. Thin foils were examined by TEM bright-field and dark-field imaging modes, selected-area electron diffraction (SAED) analysis, STEM-EDS analysis using a silicon drift detector and high-resolution high-angle annular dark-field (HAADF) imaging mode using a convergence angle of 46 mrad and detecting angles of 90–370 mrad.

Fifth, thermal stability of new phases was examined using differential scanning calorimetry (DSC) by heating the samples to 773 K with a heating rate of 5 K/min under an argon atmosphere. The samples after the DSC analysis were further examined by XRD analysis.

Sixth, the hydrogen pressure-composition isotherms (PCI) and the hydrogenation kinetics were examined in a Sieverts-type gas absorption apparatus at 303 K in the pressure range of 0.01–9 MPa for samples processed by HPT for $N = 1000$ turns. For PCI measurements, two disc samples were crushed under an argon atmosphere and subjected to evacuation at room temperature for 2 h before starting the measurements. It should be noted that the crushing was performed to increase the total surface area of the

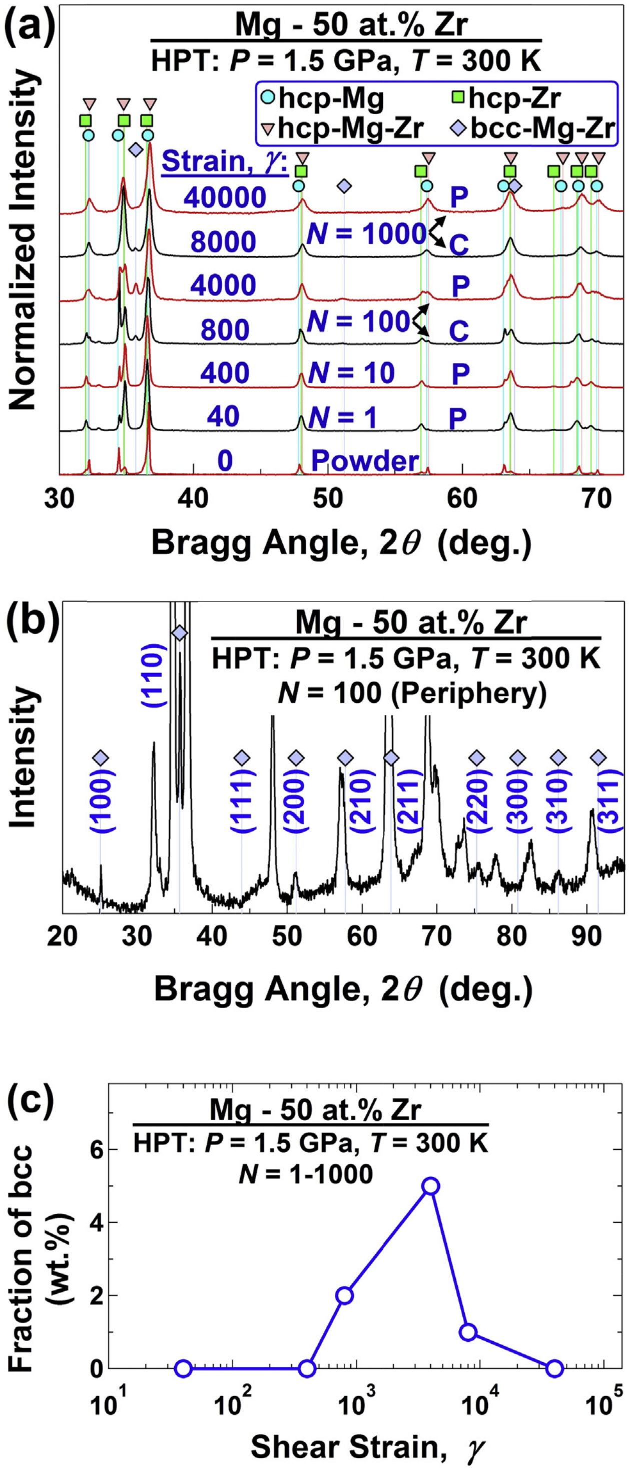

Fig. 1. (a) XRD profiles from center and periphery of discs (indicted by C and P, respectively) for samples processed by HPT for $N = 1, 10, 100$ and 1000 turns including powder mixtures; (b) XRD profile from periphery of sample processed for $N = 100$ in enlarged scale to check ordering in bcc phase; and (c) fraction of bcc phase against shear strain for samples processed by HPT for various turns.